Stereospecific Syntheses, Metal Configurational Stabilities, and Conformational Analyses of *meso*-(*R,S*)- and (*R,R*)-(η^5-C_5R_5)Ti(CH_3)$_2$-*N,N′*-bis(1-phenylethyl)acetamidinates for R = H and Me

Lisa A. Koterwas, James C. Fettinger, and Lawrence R. Sita*

Department of Chemistry and Biochemistry, University of Maryland, College Park, Maryland 20742

Received June 22, 1999

Insertion of optically pure (*R,R*)- and *meso*-(*R,S*)-1,3-bis(1-phenylethyl)carbodiimide into a Ti−C_{Me} bond of (η^5-C_5R_5)TiMe_3 provides the title compounds (*R,R*)-**3** (R = H), (*R,R*)-**5** (R = Me), (*R,S*)-**4** (R = H), and (*R,S*)-**6** (R = Me), in high yield. Reaction between (*R*)-1-*tert*-butyl, 3-(1-phenylethyl)carbodiimide, and (η^5-C_5H_5)TiMe_3 yields compound **7** in a similar fashion. Variable-temperature ^{1}H NMR studies unequivocally establish that a low-energy amidinate ring twisting pathway is the exclusive origin of configurational instability in this class of piano-stool complexes. Further, evidence for a dynamic process involving amidinate ring conformation is obtained for (*R,S*)-**6** by a similar study. A conformational analysis of the 1-phenylethyl substituents observed in the solid-state structures of (*R,R*)-**3**, (*R,R*)-**5**, *exo*-(*R,S*)-**4**, and *exo*-(*R,S*)-**6**, as determined by single-crystal X-ray analysis, provides a rationale for the apparent preferred 1-phenylethyl conformations of these compounds and of the unprecedented amidinate ring conformation (interplane angle of 41.5°) observed for the *exo* isomer of the *meso* complex **6**.

Introduction

The amidinate ligand, [N(R^1)C(R^2)N(R^3)]$^{-1}$, remains a popular group for incorporation into a wide variety of transition and main group metal complexes, as its steric and electronic effects can be manipulated through programmed variation of the substituents, R^1, R^2, and R^3.[1−3] When $R^1 \neq R^3$, there is also the ability to produce metal amidinates that are chiral at the metal center.[4,5] Accordingly, given the intense interest in the development of new chiral transition metal complexes that can serve as effective catalysts in either asymmetric organic transformations[6] or stereoselective polymerizations,[7] an elucidation of the factors that control the configurational stability of the metal center in chiral metal amidinate complexes is of paramount importance to their possible use in such roles. Recently, we reported that racemic dimethylcyclopentadienyltitanium(IV) acetamidinate complexes of the general formula (η^5-C_5R_5)TiMe_2[N(R^1)C(Me)N(R^3)] (**1**) can be prepared through facile insertion of the corresponding carbodiimides, R^1N=C=NR^3, into a Ti−C_{Me} bond of the monocyclopentadienyl starting materials, (η^5-C_5R_5)TiMe_3 (R = H and Me).[4] It was further found by ^{1}H NMR spectroscopy that in a series of these complexes where R^1 = ^{t}Bu and R^3 = Et, ^{i}Pr, and Cy (for both R = H and Me) low barriers to racemization of the titanium metal center exist as revealed by a dynamic process that exchanges the magnetic environments of the diastereotopic methyl groups bonded to titanium. As these barriers increase with increasing steric bulk of both R and R^3, it was concluded, a priori, that the mechanism by which racemization in **1** occurs is via a formal amidinate "ring-flipping" process that proceeds through a distorted trigonal bipyramidal transition state according to Scheme 1.[8] A similar dynamic process was previously proposed by Brunner, Bernal, and co-workers[5] to account for the

(1) For recent reviews, see: (a) Barker, J.; Kilner, M. *Coord. Chem. Rev.* **1994**, *133*, 219−300. (b) Edelmann, F. T. *Coord. Chem. Rev.* **1994**, *137*, 403−481.

(2) For recent studies of transition metal amidinates, see: (a) Chernega, A. N.; Gomez, R.; Green, M. L. H. *J. Chem. Soc., Chem. Commun.* **1993**, 1415−1417. (b) Gomez, R.; Green, M. L. H.; Haggitt, J. L. *J. Chem. Soc., Chem. Commun.* **1994**, 2607−2608. (c) Gomez, R.; Duchateau, R.; Chernega, A. N.; Teuben, J. H.; Edelmann, F. T.; Green, M. L. H. *J. Organomet. Chem.* **1995**, *491*, 153−158. (d) Flores, J. C.; Chien, J. C. W.; Rausch, M. D. *Organometallics* **1995**, *14*, 1827−1833. (e) Walther, D.; Fischer, R.; Gorls, H.; Koch, J.; Schweder, B. *J. Organomet. Chem.* **1996**, *508*, 13−22. (f) Dawson, D. Y.; Arnold, J. *Organometallics* **1997**, *16*, 1111−1113. (g) Hagadorn, J. R.; Arnold, J. *Inorg. Chem.* **1997**, *36*, 132−133. (h) Stewart, P. J.; Blake, A. J.; Mountford, P. *Inorg. Chem.* **1997**, *36*, 3616−3622. (i) Simpson, R. D.; Marshall, W. J. *Organometallics* **1997**, *16*, 3719−3722. (j) Hagadorn, J. R.; Arnold, J. *J. Chem. Soc., Dalton Trans.* **1997**, 3087−3096. (k) Richter, J.; Edelmann, F. T.; Noltemeyer, M.; Schmidt, H.-G.; Shmulinson, M.; Eisen, M. S. *J. Mol. Catal.* **1998**, *130*, 149−162. (l) Brandsma, M. J. R.; Brussee, E. A. C.; Meetsma, A.; Hessen, B.; Teuben, J. H. *Eur. J. Inorg. Chem.* **1998**, 1867−1870. (m) Hagadorn, J. R.; Arnold, J. *Organometallics* **1998**, *17*, 1355−1368. (n) Hagadorn, J. R.; Arnold, J. *Angew. Chem., Int. Ed. Engl.* **1998**, *37*, 1729−1731. (o) Stewart, P. J.; Blake, A. J.; Mountford, P. *Organometallics* **1998**, *17*, 3271−3281. (p) Stewart, P. J.; Blake, A. J.; Mountford, P. *J. Organomet. Chem.* **1998**, *564*, 209−214. (q) Volkis, V.; Shmulinson, M.; Averbuj, C.; Lisovskii, A.; Edelmann, F. T.; Eisen, M. S. *Organometallics* **1998**, *17*, 3155−3157. (r) Littke, A.; Sleiman, N.; Bensimon, C.; Richeson, D. S.; Yap, G. P. A.; Brown, S. J. *Organometallics* **1998**, *17*, 446−451. (s) Averbuj, C.; Tish, E.; Eisen, M. S. *J. Am. Chem. Soc.* **1998**, *120*, 8640−8646. (t) Brussee, E. A. C.; Meetsma, A.; Hessen, B.; Teuben, J. H. *Organometallics* **1998**, *17*, 4090−4095. (u) Boere, R. T.; Klassen, V.; Wolmershauser, G. *J. Chem. Soc., Dalton Trans.* **1998**, 4147−4154.

10.1021/om990481z CCC: $15.00
Publication on Web 09/10/1999

Scheme 1

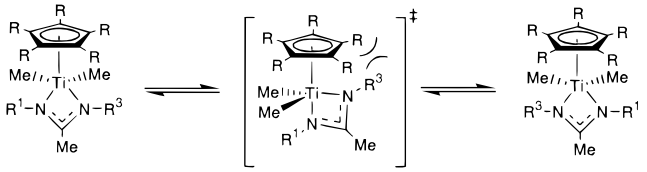

metal-centered epimerization that occurs in diastereomeric dicarbonylcyclopentadienylmolybdenum benzamidinate complexes of the general formula $CpMo(CO)_2[N(R^1)C(Ph)N(R^3)]$ [Cp = (η^5-C_5H_5)] (**2**), where R^1 and R^3 are either (*R*)- or (*S*)-1-phenylethyl. Unfortunately, in both classes of complex, **1** and **2**, neither the NMR nor the stereochemical features allow one to unequivocally establish that amidinate ring-flipping is the exclusive mechanism by which racemization/epimerization of the metal center occurs. Hence, although remote, leakage through a competitive mechanism for racemization/epimerization involving dynamic exchange of the respective diastereotopic methyl or carbonyl substituents in these complexes must still be ruled out.

To provide additional insight regarding the configurational stability of **1**, and the factors that might be used to control this process, a systematic study of new derivatives bearing chiral *N*-1-phenylethyl substituents on the amidinate ligand was undertaken. Herein, we now report the significant results of this investigation which establish that amidinate ring-flipping is indeed the operative racemization/epimerization mechanism in **1**. Further, from a series of crystal structures of the title compounds, a rationale for the preferred conformations of the 1-phenylethyl substituents of these complexes in the solid state, and possibly in solution, has been formulated. This last result is of some significance given that derivatives of **1** have been shown to be catalyst precursors for the Ziegler−Natta polymerization of ethylene upon activation with methylaluminoxane (MAO)[4,9] and that the interconversion of chiral/*meso* conformations of cationic metallocene polymerization active sites is proposed to play the key role in the production of elastomeric isotactic−atactic stereoblock polypropylene.[7,10]

Scheme 2

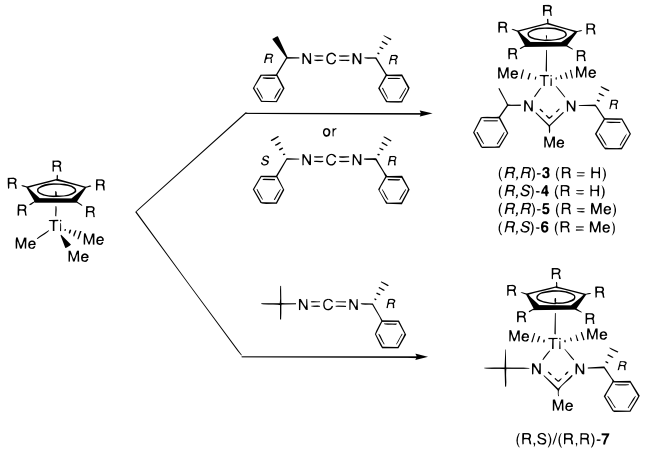

(*R*,*R*)-**3** (R = H)
(*R*,*S*)-**4** (R = H)
(*R*,*R*)-**5** (R = Me)
(*R*,*S*)-**6** (R = Me)

(R,S)/(R,R)-**7**

Results and Discussion

As shown in Scheme 2, the new titanium(IV) acetamidinates, **3**−**6**, were prepared in high yield through insertion of the corresponding carbodiimide into a Ti−C_{Me} bond of either of the two trimethylmonocyclopentadienyltitanium starting materials, $CpTiMe_3$ or Cp^*TiMe_3 ($Cp^* = \eta^5$-C_5Me_5). The requisite carbodiimides themselves were conveniently prepared through a zinc-mediated heterocumulene metathesis process that has been found to efficiently couple a monosilylated primary amine with a benzylisocyanate to afford the desired carbodiimide in high yield.[11,12] In cases where $CpTiMe_3$ was utilized, the insertion reaction proceeded rapidly at room temperature to provide the titanium amidinate products as dark red solids that could be obtained in analytically pure form after recrystallization from pentane at −35 °C. For complete formation of the pentamethylcyclopentadienyltitanium amidinates, however, it was found that much longer reaction times were required (e.g., ∼18 h) to obtain the compounds in high yield as orange-red crystalline solids that could once more be recrystallized from pentane at −35 °C. Finally, as an extension of the previously prepared homologous series of *tert*-butyl-substituted derivatives of **1**,[4] compound **7** was prepared in high yield from $CpTiMe_3$ and (*R*)-1-*tert*-butyl-3-(1-phenylethyl)carbodiimide according to Scheme 2.

To establish that amidinate ring-flipping is the exclusive mechanism for racemization/epimerization in **1**, variable-temperature ^{1}H NMR studies of the optically active derivatives (*R*,*R*)-**3** and (*R*,*R*)-**5** were undertaken. When performed for **3**, a single set of resonances for the 1-phenylethyl substituents was observed at room temperature. Surprisingly, however, no decoalescence to two sets of resonances for these formally diastereotopic

(3) For recent studies of main group metal amidinates, see: (a) Zhou, Y.; Richeson, D. S. *Inorg. Chem.* **1996**, *35*, 2448−2451. (b) Zhou, Y.; Richeson, D. S. *J. Am. Chem. Soc.* **1996**, *118*, 10850−10852. (c) Zhou, Y.; Richeson, D. S. *Inorg. Chem.* **1996**, *35*, 1423−1424. (d) Foley, S. R.; Bensimon, C.; Richeson, D. S. *J. Am. Chem. Soc.* **1997**, *119*, 10359−10363. (e) Coles, M. P.; Swenson, D. C.; Jordan, R. F.; Young, V. G., Jr. *Organometallics* **1997**, *16*, 5183−5194. (f) Coles, M. P.; Jordan, R. F. *J. Am. Chem. Soc.* **1997**, *119*, 8125−8126. (g) Zhou, Y.; Richeson, D. S. *Inorg. Chem.* **1997**, *36*, 501−504. (h) Coles, M. P.; Swenson, D. C.; Jordan, R. F. *Organometallics* **1998**, *17*, 4042−4048. (i) Karsch, H. H.; Schluter, P. A.; Reisky, M. *Eur. J. Inorg. Chem.* **1998**, 433−436.

(4) Sita, L. R.; Babcock, J. R. *Organometallics* **1998**, *17*, 5228−5230.

(5) (a) Brunner, H.; Agrifoglio, G.; Bernal, I.; Creswick, M. W. *Angew. Chem., Int. Ed. Engl.* **1980**, *19*, 641−642. (b) Brunner, H.; Agrifoglio, G. *J. Organomet. Chem.* **1980**, *202*, C43−C48. (c) Brunner, H.; Lukassek, J.; Agrifoglio, G. *J. Organomet. Chem.* **1980**, *195*, 63−76. (d) Brunner, H.; Agrifoglio, G.; Benn, R.; Rufinska, A. *J. Organomet. Chem.* **1981**, *217*, 365−371.

(6) *Catalytic Asymmetric Synthesis*; Ojima, I., Ed.; VCH Publishers: New York, 1993.

(7) Brintzinger, H. H.; Fischer, D.; Mulhaupt, R.; Rieger, B.; Waymouth, R. M. *Angew. Chem., Int. Ed. Engl.* **1995**, *34*, 1143−1170.

(8) A dissociative mechanism has been proposed as the pathway for equilibration of diastereotopic substituents in other classes of metal amidinates; see: (a) Wedler, M.; Knosel, F.; Edelmann, F. T.; Behrens, U. *Chem. Ber.* **1992**, *125*, 1313−1318. (b) Stewart, P. J.; Blake, A. J.; Mountford, P. *Organometallics* **1998**, *17*, 3271−3281.

(9) Green and co-workers[2a−c] have also shown that zirconium analogues of **1** can serve as catalyst precursors for Ziegler−Natta polymerization.

(10) (a) Coates, G. W.; Waymouth, R. M. *Science* **1995**, *267*, 217. (b) Petoff, J. L. M.; Agoston, T.; Lal, T. K.; Waymouth, R. M. *J. Am. Chem. Soc.* **1998**, *120*, 11316−11322.

(11) Babcock, J. R.; Sita, L. R. Syntheses to be published elsewhere.

(12) For a previous synthesis of unsymmetric carbodiimides using a tin(II)-mediated heterocumulene process, see: Babcock, J. R.; Sita, L. R. *J. Am. Chem. Soc.* **1998**, *120*, 5585−5587. Unfortunately, for benzylisocyanates, this method leads to poor results due to a competitive tin(II)-catalyzed polymerization of this particular class of starting material.

Scheme 3

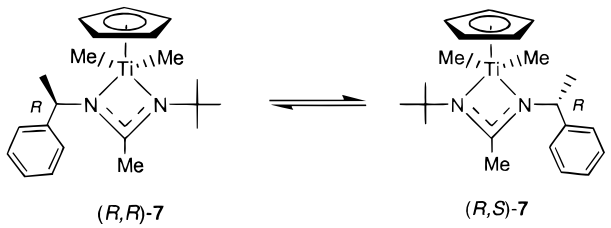

substituents could be observed even down to a temperature of 173 K, thereby suggesting that a much lower barrier to epimerization exists in this complex than in the previously studied series of *tert*-butyl-substituted derivatives of **1**.[4] What the peculiar steric and electronic effects of the 1-phenylethyl substituent are on this energy barrier is still under investigation at the present time. However, with respect to the present study, what is important is that, at all temperatures and up to the decomposition temperature of 333 K, two distinct quartets (^4J = 1.1 Hz) for the diastereotopic methyl groups that are directly bonded to the titanium center in **3** could be observed. Further, a set of 2D EXSY ^{1}H NMR[13] spectra of **3**, taken at 333 K using a range of mixing times, failed to display any exchange cross-peaks between the two methyl resonances, thus making the existence of dynamic methyl group exchange as a competitive mechanism for racemization/epimerization highly unlikely (see also below for **7**). Additional support for this conclusion was provided by the set of variable-temperature ^{1}H NMR spectra for (*R,R*)-**5**. Hence, as with **3**, two distinct resonances for the diastereotopic methyl groups bonded to titanium in this complex were observed at all temperatures. However, due to the increased barrier to racemization/epimerization that is provided by the more sterically encumbered Cp* ligand, upon cooling, the single set of (broad) resonances for the diastereotopic 1-phenylethyl substituents observed at room temperature now decoalesced to two sharp sets of resonances at the slow exchange limit of 223 K.[14] At the coalescence temperature, T_c, of 263 K, an approximate value of $\Delta G^{\ddagger}$ for this process was calculated to be only 12.3 kcal mol^{-1}, which is significantly low when compared to values previously obtained for *tert*-butyl-substituted derivatives of **1**.[4] Certainly, one possible reason for this lower barrier is due to the reduction in steric interactions that occurs upon replacement of a *tert*-butyl by a 1-phenylethyl substituent. In fact, a variable-temperature ^{1}H NMR study of **7** provided evidence for a higher barrier for epimerization between the two possible (*R,R*) and (*R,S*) diastereomeric complexes (see Scheme 3) even though this is only a Cp-substituted derivative as compared to **5**. Interestingly, however, even at the *apparent* slow exchange limit of 213 K, a 2D EXSY ^{1}H NMR spectrum of the Cp resonances of **7** revealed that substantial dynamic exchange via amidinate ring-flipping is still occurring between the two diastereomers, as supported by the magnitude of the exchange cross-peaks that are shown in Figure 1. Finally, although achiral, two diastereomers for each of the *meso* complexes, **4** and **6**, can exist due to an asymmetry in the plane, which is orthogonal to

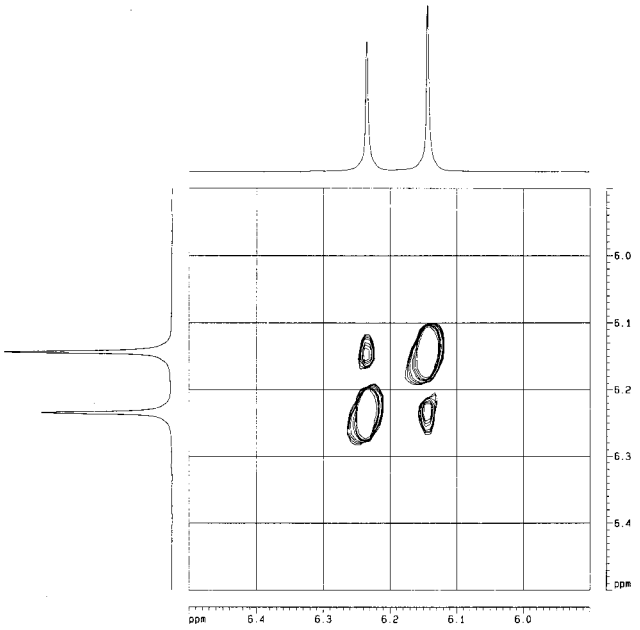

Figure 1. 2D EXSY ^{1}H NMR (500 MHz, toluene-d_8) spectrum of the cyclopentadienyl resonances of (*R,S*)/(*R,R*)-**7** recorded at 213 K with a mixing time of 350 ms.

Scheme 4

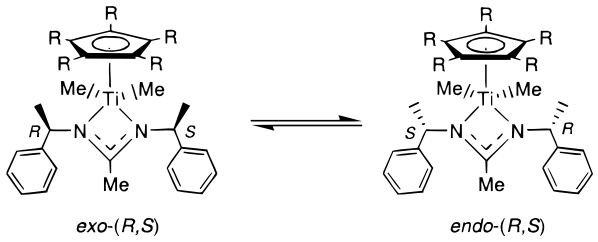

the mirror plane, which makes the 1-phenylethyl substituents "externally diastereotopic".[15] Accordingly, complete variable-temperature ^{1}H NMR studies of (*R,S*)-**4** and (*R,S*)-**6** were conducted to determine if the expected dynamic exchange process between these two diastereomers, hereafter designated the *exo* and the *endo* isomers according to Scheme 4, could be observed. In the case of **4**, two sets of resonances for the *exo* and *endo* isomers, which could not be unequivocally assigned to either isomer, but which were present in a ~1.2:1 ratio, could indeed be resolved at the low temperature of 173 K, which, however, does not represent the slow exchange limit for exchange [T_c = 198 K for the Cp resonances at 5.62 ppm (major isomer) and 6.13 ppm (minor)]. In contrast, due to the increased steric interactions of the Cp* ligand, the set of variable-temperature spectra for **6** now revealed that the apparent slow exchange limit for dynamic exchange between the *exo* and *endo* isomers could be established at the higher temperature of 233 K, where two sets of resonances in a 1.4:1 ratio are observed. Interestingly, upon cooling below this temperature, another dynamic process begins to selectively broaden the resonances for one of these isomers over the other, as Figure 2 reveals. A proposal

(13) Braun, S.; Kalinowski, H.-O.; Berger, S. *100 and More Basic NMR Experiments*; VCH Publishers: New York, 1996.

(14) Detailed information is provided in the Supporting Information.

(15) For a discussion of this form of stereoisomerism, see: Eliel, E. L.; Wilen, S. H. *Stereochemistry of Organic Compounds*; John Wiley & Sons: New York, 1994; pp 493−494. For a recent example in an inorganic complex, see: Mattamana, S. P.; Promprai, K.; Fettinger, J. C.; Eichhorn, B. W. *Inorg. Chem.* **1998**, *37*, 6222−6228.

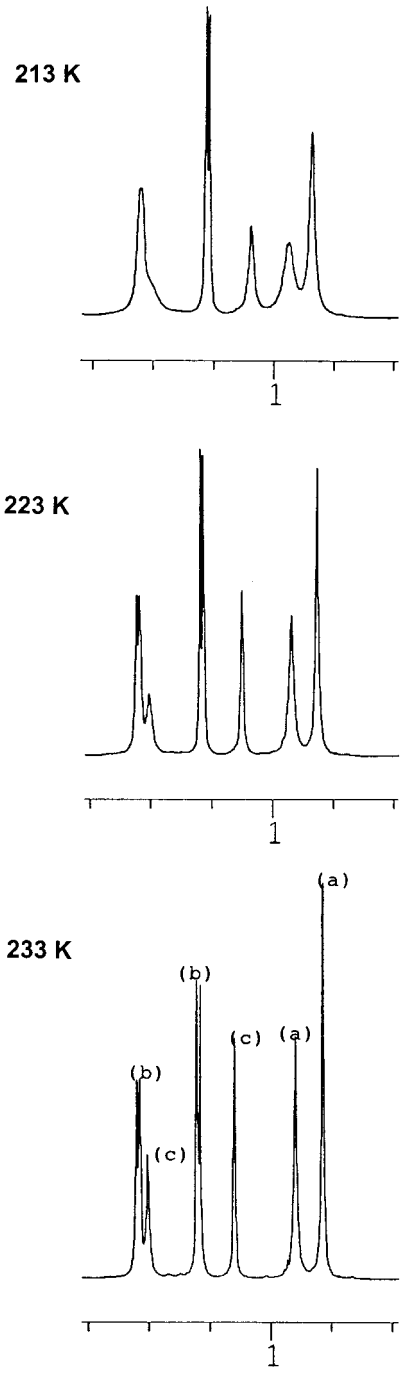

Figure 2. Variable-temperature ^{1}H NMR (500 MHz, toluene-d_8) spectra for the upfield methyl resonances of *exo*/*endo*-(*R*,*S*)-**6**. Assignments are (a) Ti−CH_3, (b) Ph−CH-(CH_3)−N, (c) N−C(CH_3)−N.

for the origin of this new dynamic process will be discussed shortly.

To determine whether the origin of the low configurational stabilities of **3**−**6** also manifests itself in the structural parameters of these compounds, single-crystal X-ray analyses were conducted.[14] Table 1 provides a listing of the crystal structure and refinement data, Tables 2−4 show selected bond distances and angles, and Figures 3−6 show the molecular structures of **3**−**6**. As can be noted in the latter, the titanium amidinate complexes are all monomeric in the solid state. It is also important to point out that for each of the *meso* complexes, **4** and **6**, which, as mentioned, can

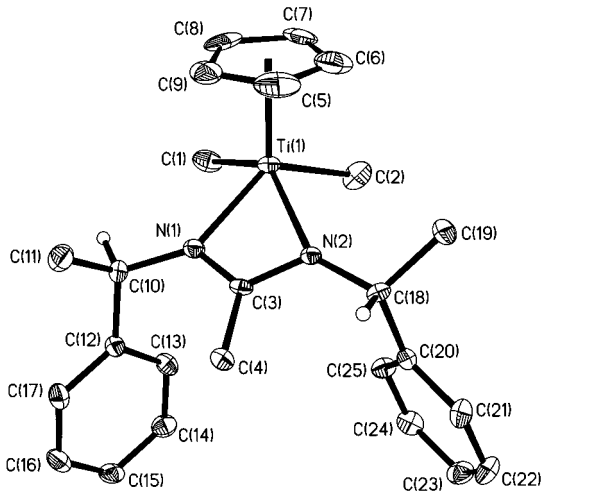

Figure 3. ORTEP representation (30% thermal ellipsoids) of the molecular structure of (*R*,*R*)-**3**. Hydrogen atoms have been removed for the sake of clarity except for those represented by spheres of arbitrary size that are located on the carbon atom of chiral centers.

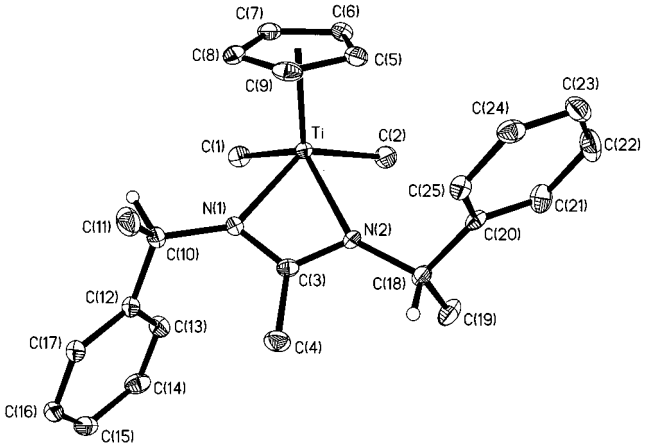

Figure 4. ORTEP representation (30% thermal ellipsoids) of the molecular structure of *exo*-(*R*,*S*)-**4**. Hydrogen atoms have been removed for the sake of clarity except for those represented by spheres of arbitrary size that are located on the carbon atom of chiral centers.

exist as either *exo* or *endo* isomers, only crystals of the *exo* isomers were obtained for analysis. Whether this selectivity is the result of preferential crystallization of the *exo* over the *endo* isomers or the product of pure happenstance awaits further efforts to obtain the pure *endo* isomers in crystalline form.

In the absence of a crystallographic mirror plane, such as that found for **6**, it can be seen upon inspection of Table 2, that the amidinate metallacycles of compounds **3**−**5** are all asymmetric with respect to their internal bond distances. Thus, in each case, the Ti−N(1) bond distances are found to be significantly shorter than the corresponding Ti−N(2) values [cf. **3**, 2.098(4) Å vs 2.159(4) Å; **4**, 2.121(2) Å vs 2.153(2) Å; **5**, 2.114(2) Å vs 2.157(2) Å]. A comparison with other titanium amidinate crystal structures reveals that such amidinate ring asymmetry is the norm rather than the exception for titanium(IV) complexes, although the magnitude of the differences between these two sets of Ti−N bond lengths is still somewhat surprising given the absence of differing *trans* ligand influences.[1,2] It can also be noted

Table 1. Crystal Structure and Refinement Data for Compounds 3−6

	3	4	5	6
formula	$C_{25}H_{32}N_2Ti$	$C_{25}H_{32}N_2Ti$	$C_{30}H_{42}N_2Ti$	$C_{30}H_{42}N_2Ti$
M_w	408.43	408.43	478.56	478.56
space group	orthorhombic *P*2(1)2(1)2(1)	monoclinic *P*2(1)/*n*	orthorhombic *P*2(1)2(1)2(1)	orthorhombic *Pnma*
a (Å)	9.2223(8)	15.0097(8)	11.8784(8)	11.9760(13)
b (Å)	13.0585(15)	9.4233(6)	12.2742(10)	17.2131(14)
c (Å)	18.533(2)	17.0435(11)	18.6114(14)	13.0330(11)
β (deg)	90	114.807(5)	90	90
V (Å^3)	2231.9(4)	2188.2(2)	2713.5(4)	2686.7(4)
Z	4	4	4	4
D_{calcd} (Mg/m^3)	1.215	1.240	1.171	1.183
abs coeff (mm^{-1})	0.395	0.403	0.335	0.338
F(000)	872	872	1032	1032
crystal size, mm^3	0.50 × 0.35 × 0.10	0.22 × 0.22 × 0.18	0.33 × 0.27 × 0.24	0.40 × 0.26 × 0.27
θ range (deg)	2.47−25.00	2.37−24.98.	2.19−27.56	2.31−25.00
no. of reflns collected	8299	3978	10280	4899
no. of ind reflns	3906 (R_{int} = 0.1110)	3841 (R_{int} = 0.0373)	6229 (R_{int} = 0.0568)	2451 (R_{int} = 0.0409)
abs corr	integration	integration	integration	empirical
transmission range	0.8268−0.9615	0.9165−0.9309	0.9128−0.9303	0.8157−0.8830
refinement method	full-matrix least-squares on F^2			
goodness of fit on F^2	1.073	1.014	1.035	1.051
final *R* indices [$I > 2\sigma(I)$]	R1 = 0.0533 wR2 = 0.1235	R1 = 0.0458 wR2 = 0.0929	R1 = 0.0455 wR2 = 0.0919	R1 = 0.0417 wR2 = 0.0889

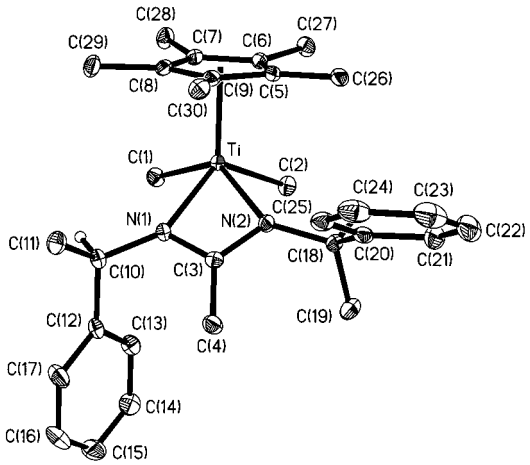

Figure 5. ORTEP representation (30% thermal ellipsoids) of the molecular structure of (*R,R*)-**5**. Hydrogen atoms have been removed for the sake of clarity except for those represented by spheres of arbitrary size that are located on the carbon atom of chiral centers.

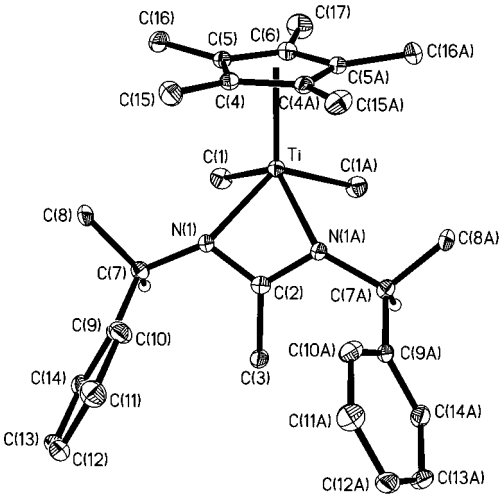

Figure 6. ORTEP representation (30% thermal ellipsoids) of the molecular structure of *exo*-(*R,S*)-**6**. Hydrogen atoms have been removed for the sake of clarity except for those represented by spheres of arbitrary size that are located on the carbon atom of chiral centers.

that, except for **5**, the "direction" in asymmetry found for the corresponding N(1)−C(3) and N(2)−C(3) bond distances within the metallacycles [cf. **3**, 1.323(5) Å vs 1.341(5) Å; **4**, 1.323(4) Å vs 1.330(4) Å; **5**, 1.339(3) Å vs 1.325(3) Å] does not fit with that expected for a classic unsymmetric σ,σ chelating mode of amidinate ligand bonding in which one nitrogen atom formally bonds to the metal center via an imine lone pair of electrons.[1a] Finally, with respect to bond distances, curious differences in the Ti−C(1) and Ti−C(2) bond length values are found for compounds **4** and **5** [cf. **4**, 2.123(3) Å vs 2.144(3) Å and **5**, 2.154(3) Å vs 2.116(3) Å]. As the direction of this Ti−C_{Me} bond length difference is opposite between the two complexes, no readily apparent explanation can be found at this level of investigation. Collectively, however, the bond length differences observed within compounds **3**−**5** are suggestive of a rather "soft" ground-state energy potential for this class of complex which can accommodate a range of structural distortions.

In contrast to bond lengths, an analysis of the bond angles found within compounds **3**−**6** offers few surprises (see Table 3). As expected, the small bite of the chelating amidinate ring establishes N−Ti−N bond angles of 61−62°, which are within the previously observed range.[1−3] The other endocyclic amidinate bond angles, and those involving the titanium center within the distorted square-pyramidal structure, are also in agreement with those anticipated from the types of geometrical constraints placed on the structure. Finally, in each compound, the Ti−N−C bond angles that are external to the metallacycle are within the range 136−148°, and this is, once more, in keeping with known metal amidinate complexes that possess bulky N-substituents.[1−3]

Although the bond distances and bond angles for compounds **3**−**6** all fall within expected ranges, a striking structural feature of **6** can be found by considering the conformations that all of these compounds adopt in the solid state. Thus, as Table 4 reveals, the carbon and nitrogen atoms within the amidinate ligands of **3** and **4** [i.e., C(3), N(1), and N(2)] are all strictly

Table 2. Selected Bond Distances (Å) for Compounds 3−6

				Compound **3**					
Ti−Cp_{cent}[a]	2.049(3)	Ti−C(7)	2.385(5)	Ti−C(1)	2.133(5)	Ti−N(2)	2.159(4)	N(2)−C(3)	1.341(5)
Ti−C(5)	2.347(5)	Ti−C(8)	2.365(6)	Ti−C(2)	2.131(4)	N(1)−C(3)	1.323(5)	N(2)−C(18)	1.459(5)
Ti−C(6)	2.383(6)	Ti−C(9)	2.327(6)	Ti−N(1)	2.098(4)	N(1)−C(10)	1.467(5)	C(3)−C(4)	1.506(6)
				Compound **4**					
Ti− Cp_{cent}[a]	2.055(2)	Ti−C(7)	2.379(3)	Ti−C(1)	2.123(3)	Ti−N(2)	2.153(2)	N(2)−C(3)	1.330(4)
Ti−C(5)	2.367(3)	Ti−C(8)	2.381(3)	Ti−C(2)	2.144(3)	N(1)−C(3)	1.323(4)	N(2)−C(18)	1.467(4)
Ti−C(6)	2.372(3)	Ti−C(9)	2.367(3)	Ti−N(1)	2.121(2)	N(1)−C(10)	1.471(4)	C(3)−C(4)	1.501(4)
				Compound **5**					
Ti− Cp_{cent}[a]	2.0639(17)	Ti−C(7)	2.401(3)	Ti−C(1)	2.154(3)	Ti−N(2)	2.157(2)	N(2)−C(3)	1.325(3)
Ti−C(5)	2.391(3)	Ti−C(8)	2.378(2)	Ti−C(2)	2.116(3)	N(1)−C(3)	1.339(3)	N(2)−C(18)	1.466(3)
Ti−C(6)	2.400(3)	Ti−C(9)	2.379(3)	Ti−N(1)	2.114(2)	N(1)−C(10)	1.474(3)	C(3)−C(4)	1.500(4)
				Compound **6**					
Ti− Cp_{cent}[a]	2.071(2)	Ti−C(6)	2.415(4)	N(1)−C(2)	1.337(3)				
Ti−C(4)	2.372(2)	Ti−C(1)	2.141(3)	N(1)−C(7)	1.471(3)				
Ti−C(5)	2.409(2)	Ti−N(1)	2.1548(19)	C(2)−C(3)	1.511(5)				

[a] Cp_{cent} = calculated centroid of cyclopentadienyl ligand.

Table 3. Selected Bond Angles (deg) for Compounds 3−6

			Compound **3**				
C(2)−Ti(1)−C(1)	86.73(19)	C(2)−Ti(1)−N(2)	90.5(2)	C(3)−N(1)−C(10)	124.0(4)	C(3)−N(2)−C(18)	120.8(3)
N(1)−Ti(1)−N(2)	62.10(15)	C(3)−N(1)−Ti(1)	94.8(2)	C(3)−N(2)−Ti(1)	91.6(2)	N(1)−C(3)−N(2)	111.1(4)
N(1)−Ti(1)−C(1)	83.40(18)	C(10)−N(1)−Ti(1)	141.2(3)	C(18)−N(2)−Ti(1)	147.5(3)	N(1)−C(3)−C(4)	126.4(4)
						N(2)−C(3)−C(4)	122.6(4)
			Compound **4**				
C(1)−Ti−C(2)	87.63(16)	C(2)−Ti−N(2)	87.29(13)	C(3)−N(1)−C(10)	125.8(3)	C(3)−N(2)−C(18)	121.7(2)
N(1)−Ti−N(2)	61.56(9)	C(3)−N(1)−Ti	94.53(18)	C(3)−N(2)−Ti	92.89(17)	N(1)−C(3)−N(2)	111.0(3)
N(1)−Ti−C(1)	86.17(12)	C(10)−N(1)−Ti	139.3(2)	C(18)−N(2)−Ti	145.4(2)	N(1)−C(3)−C(4)	124.9(3)
						N(2)−C(3)−C(4)	124.1(3)
			Compound **5**				
C(1)−Ti−C(2)	87.56(13)	C(2)−Ti−N(2)	86.48(10)	C(3)−N(1)−C(10)	124.7(2)	C(3)−N(2)−C(18)	125.7(2)
N(1)−Ti−N(2)	61.27(8)	C(3)−N(1)−Ti	94.91(15)	C(3)−N(2)−Ti	93.36(15)	N(1)−C(3)−N(2)	109.6(2)
N(1)−Ti−C(1)	85.51(10)	C(10)−N(1)−Ti	139.56(17)	C(18)−N(2)−Ti	136.26(16)	N(1)−C(3)−C(4)	125.1(2)
						N(2)−C(3)−C(4)	125.3(2)
			Compound **6**				
C(1)−Ti−C(1A)	84.09(18)	N(1A)−Ti−C(1A)	84.76(10)	C(2)−N(1)−C(7)	119.68(19)	N(1)−C(2)−C(3)	124.15(14)
N(1)−Ti−N(1A)	61.67(10)	C(2)−N(1)−Ti	86.50(16)	N(1)−C(2)−N(1A)	111.4(3)		
N(1)−Ti−C(1)	84.76(10)	C(7)−N(1)−Ti	137.89(16)	N(1)−C(2)−C(3)	124.15(14)		

Table 4. Selected Sum of Bond Angles, Torsion Angles, and Interplane Angles (deg) for Compounds 3−6

	3	4	5	6
Sum of Angles ($\Sigma\theta$)				
N(1)	360.0	359.9	359.2	344.1
N(2)	359.5	360.0	355.3	
C(3)[a]	360.0	360.0	360.0	360.0
Torsion Angles[b]				
C(3)−N(1)−C(10)−H(10)[c]	−171.1	−178.7	−160.0	−64.4
C(3)−N(2)−C(18)−H(18)	−41.0	−17.7	+159.9	
Interplane Angles				
N(1)−C(3)−N(2) and N(1)−Ti−N(2)[d]	7.2	0.4	9.8	41.5

[a] C(2) in the case of **6**. [b] For a torsion angle defined by $i-j-k-l$, sign conventions are (+) if a clockwise and (−) if a counterclockwise rotation of the $i-j$ bond vector is required to bring it inline with the $k-l$ vector as one views along the $j-k$ vector. [c] C(2)−N(1)−C(7)−H(7) in the case of **6**. [d] N(1)−C(2)−N(1A) and N(1)−Ti−N(1A) in the case of **6**.

trigonal coplanar. In compound **5**, this trend is continued except for N(2), which now displays a slight pyramidal distortion [cf. $\Sigma\theta_{N(2)} = 355.3°$]. Upon closer inspection of the molecular structure of **5** that is shown in Figure 5, it can be seen that the (*R*)-1-phenylethyl substituent of N(2) is in close proximity to the methyl groups of the Cp* ligand [cf. the closest nonbonded distance between the hydrogen atoms of C(26) and the calculated centroid of the phenyl ring comprised of C(20)−C(25) of 3.262 Å]. Accordingly, the pyramidal distortion that is observed for N(2) in **5** most likely arises from nonbonded steric interactions. Probing further, a comparison of the degree of nonplanarity of the amidinate metallacycles in compounds **3**−**5**, as determined by the angle between the planes defined by N(1)−Ti−N(2) and N(1)−C(3)−N(2), shows that these four-membered rings are either essentially planar, as in the case of **4**, or slightly puckered, as found for **3** and **5** (interplane angles of 7.2° and 9.8°, respectively). While the vast majority of metal amidinate structures do possess planar amidinate metallacycles, a few are nonplanar, with corresponding interplane angles of between 0.1 and 11.5° being typically observed for those mononuclear metal amidinate structures for which this parameter has been reported.[1−3] Overall then, while the solid-state structures found for **3**−**5** in the present study appear to be quite normal, such is not the case for compound **6** since, as Table 4 reveals, the degree of nonplanarity found for the amidinate metallacycle in this complex is quite severe, as determined by the strikingly large interplane angle of 41.5° and the substantial pyramidalization of the nitrogen atoms [$\Sigma\theta_{N(1)} = 344.1°$] that are observed. Figure 7 presents a side view of the molecular structure of **6** in which the extent of this nonplanarity of the amidinate group can be better appreciated. Importantly, to the best of our knowledge, no other mononuclear metal amidinate

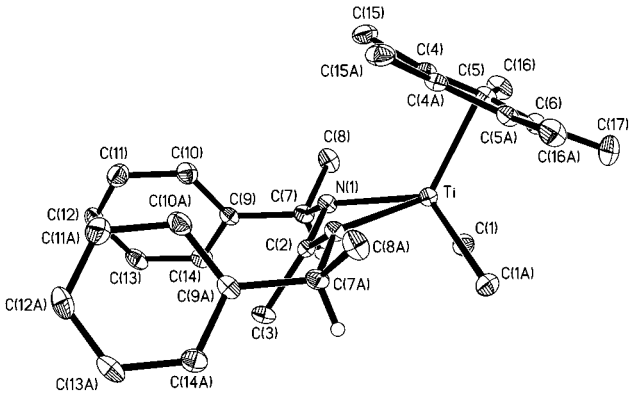

Figure 7. ORTEP representation (30% thermal ellipsoids) of a side view, with respect to Figure 6, of the molecular structure of *exo*-(*R,S*)-**6**. Hydrogen atoms have been omitted for clarity.

Scheme 5

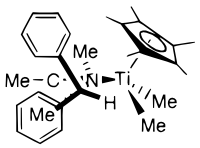

(*R,R*)-**5**

complex has yet been found that adopts such a strongly puckered amidinate ring conformation in the solid state.

In an attempt to provide a rationalization for why only **6** adopts a severely distorted amidinate ring structure, an analysis of the possible factors directing the preferred solid-state conformations of the *N*-1-phenylethyl substituents of **3**−**6** yielded three key observations. These are as follows.

(1) The lowest energy conformation of a *single* 1-phenylethyl substituent appears to be one in which the bond between the amidinate carbon atom and its substituent bisects the $C_{Me}-C-C_{Ph}$ bond angle *and* in which the phenyl group is directed away from the Cp or Cp* ligand. Whether a 1-phenylethyl substituent can adopt this conformation is governed by its absolute configuration.

(2) For Cp derivatives, only one instance of a conformation of type (1) is allowed. A second 1-phenylethyl substituent must, therefore, adopt the next energetically favored conformation, in which the hydrogen atom of the substituent is nearly coplanar with, and directed toward, the carbon atom of the amidinate ring. The absolute configuration of this second substituent then dictates whether its phenyl group is directed toward, and in close contact with, the Cp ring or away from it.

(3) In Cp* derivatives, conformations of type (2) are not allowed due to strong steric interactions. In this case, two conformations of type (1) are preferred, as found in the structure of (*R,R*)-**5** that is schematically redrawn in Scheme 5.

The observations enumerated above can be used to make predictions regarding the preferred solution conformations of **3**−**6**. For instance, there is now a sound basis to believe that the chiral conformation observed for *exo*-**4** in the solid state is also the lowest energy conformation in solution. Accordingly, efforts are in progress to determine if the rate of interconversion between *meso* and racemic conformations of **1** can be

Scheme 6

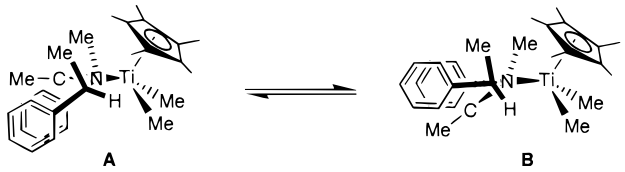

directly controlled through the use of substituents in a manner similar to that implemented by Waymouth and co-workers[10] involving zirconium metallocenes. The above observations also allow us to propose a hypothesis regarding the unusual structure of the *meso* complex (*R,S*)-**6**. Thus, according to the last observation, conformation **A** in Scheme 6 is predicted to be the preferred one. However, placement of the two phenyl rings in this configuration now establishes a significant barrier to the amidinate ring conformational change between **A** and **B** that is shown. Accordingly, we believe it is this barrier that establishes the new dynamic process that is observed by ^{1}H NMR spectroscopy at very low temperatures for the *exo* isomer of **6**. This barrier also then provides an explanation of the unusual solid-state conformation of the *exo* isomer of **6**, which is essentially locked into place by the two phenyl rings.

Conclusion

Carbodiimide insertion into Ti−C bonds provides a convenient and efficient manner by which to produce a variety of derivatives of **1**. The present study has served to further clarify the origin of configurational instability in this class of compound, as well as to provide a set of observations that might be used to manipulate this instability for further use. Importantly, we document new types of conformational and stereochemical complexities that exist for the amidinate ligand, and this information may aid in the future design of effective catalysts that employ this group.

Experimental Section

All manipulations were performed under an inert atmosphere of nitrogen using standard Schlenk and/or glovebox techniques. All solvents were dried and distilled under nitrogen prior to use. $CpTiMe_3$ and Cp^*TiMe_3 were prepared according to the literature procedure.[16] ^{1}H NMR spectra were recorded at 400 or 500 MHz using toluene-d_8 as the solvent. Chemical analyses were performed by Midwest Micolab.

General Synthetic Procedure. In a glovebox, a solution of 1 mmol of either $CpTiMe_3$ or Cp^*TiMe_3 in 1 mL of pentane was placed inside a vial and a solution of 1 mmol of the carbodiimide in 1 mL of pentane added at room temperature by pipet. After stirring overnight at this temperature, the solvent was removed in vacuo and the red, or orange-red, crystalline solid recrystallized from pentane at −35 °C to provide analytically pure material.

(*R,R*)-CpTiMe$_2$[N(1-phenylethyl)C(Me)N(1-phenylethyl)] (3). **3** was obtained as a dark red crystalline solid in a 83% yield from $CpTiMe_3$ and (*R,R*)-1,3-bis(1-phenylethyl)-carbodiimide. For **3**: ^{1}H NMR (400 MHz, 298 K, toluene-d_8) δ 0.95 (q, 3H, J = 1.1 Hz), 1.03 (q, 3H, J = 1.1 Hz), 1.33 (d, 6H, J = 7.0 Hz), 1.43 (s, 3H), 4.33 (q, 2H, J = 7.0 Hz), 6.01 (s, 5H), 7.02 (m, 2H), 7.19 (m, 4H), 7.29 (m, 4H). Anal. Calcd for

(16) Giannini, U.; Cesca, S. *Tetrahedron Lett.* **1960**, *14*, 19−20.

$C_{25}H_{32}N_2Ti$: C, 73.52; H, 7.90; N, 6.86. Found: C, 72.84; H, 7.84; N, 6.86.

***exo/endo*-(*R,S*)-CpTiMe$_2$[N(1-phenylethyl)C(Me)N(1-phenylethyl)] (4).** **4** was obtained as a dark red crystalline solid in a 76% yield from $CpTiMe_3$ and (*R,S*)-1,3-bis(1-phenylethyl)carbodiimide. For **4**: ^{1}H NMR (500 MHz, 273 K, toluene-d_8) δ 1.01 (s, 6H), 1.29 (d, 6H, J = 6.5 Hz), 1.41 (s, 3H), 4.29 (q, 2H, J = 7.0 Hz), 6.01 (s, 5H), 7.04 (t, 2H, J = 7.5 Hz), 7.165 (t, 4H, J = 7.5 Hz), 7.26 (d, 4H, J = 7.5 Hz). Anal. Calcd for $C_{25}H_{32}N_2Ti$: C, 73.52; H, 7.90; N, 6.86. Found: C, 73.16; H, 7.82; N, 6.76.

(*R,R*)-Cp*TiMe$_2$[N(1-phenylethyl)C(Me)N(1-phenylethyl)] (5). **5** was obtained as an orange-red crystalline solid in a 89% yield from Cp*$TiMe_3$ and (*R,R*)-1,3-bis(1-phenylethyl)-carbodiimide. For **5**: ^{1}H NMR (500 MHz, 288 K, toluene-d_8) δ 0.72 (br s, 3H), 0.75 (br s, 3H), 1.41 (s, 3H), 1.51 (br d, 6H), 1.92 (s, 15H), 4.44 (q, 2H, J = 7.0 Hz), 7.04 (t, 2H, J = 7.5 Hz), 7.19 (t, 4H, J = 7.5 Hz), 7.44 (br s, 4H). Anal. Calcd for $C_{30}H_{42}N_2Ti$: C, 75.29; H, 8.85; N, 5.85. Found: C, 75.15; H, 8.90; N, 5.81.

***exo/endo*-(*R,S*)-Cp*TiMe$_2$[N(1-phenylethyl)C(Me)N(1-phenylethyl)] (6).** **6** was obtained as an orange-red solid in a 90% yield from Cp*$TiMe_3$ and (*R,S*)-1,3-bis(1-phenylethyl)-carbodiimide. For **6**: ^{1}H NMR (400 MHz, 298 K, toluene-d_8) δ 0.73 (br s, 6H), 1.43 (m, 9H), 1.95 (s, 15H), 4.33 (q, 2H, J = 7.0 Hz), 7.02 (t, 2H, J = 7.5 Hz), 7.20 (t, 4H, J = 7.5 Hz), 7.44 (br s, 2H), 7.46 (br s, 2H). Anal. Calcd for $C_{30}H_{42}N_2Ti$: C, 75.29; H, 8.85; N, 5.85. Found: C, 75.01; H, 8.90; N, 6.01.

(*R,S*)/(*R,R*)-CpTiMe$_2$[N(^{t}Bu)C(Me)N(1-phenylethyl)] (7). **7** was obtained as a dark red crystalline solid in a 85% yield from $CpTiMe_3$ and (*R*)-1-*tert*-butyl-3-(1-phenylethyl)carbodiimide. For **7**: ^{1}H NMR (400 MHz, 298 K, toluene-d_8) δ 0.88 (q, 3H, J = 1.1 Hz), 0.90 (br s, 3H), 1.06 (s, 9H), 1.32 (d, 3H, J = 7.0 Hz), 1.74 (s, 3H), 4.37 (q, 1H, J = 7.0 Hz), 6.22 (s, 5H), 7.05 (t, 1H, J = 7.5 Hz), 7.18 (t, 2 H, J = 7.5 Hz), 7.36 (br s, 2H). Anal. Calcd for $C_{21}H_{32}N_2Ti$: C, 69.99; H, 8.95; N, 7.77. Found: C, 68.67; H, 8.87; N, 7.89.

Crystallography. As a general procedure, for **3**, an orange block with dimensions 0.500 × 0.350 × 0.100 mm was placed and optically centered on an Enraf-Nonius CAD-4 diffractometer that was controlled by a Digital Equipment Corporation MicroVAX II (MVII) computer and the Enraf-Nonius VAX\VMS CAD4 Express control program.[17] The crystal's final cell parameters and crystal orientation matrix were determined from 25 reflections in the range 8.4° < θ < 16.3°; these constants were confirmed with axial photographs. Data were collected [Mo Kα, 153(2) K] with $\omega/2\theta$ scans over the range 2.5° < θ < 25.0° with a scan width of (0.88 + 1.00 tan θ)° and variable scan speed of 2.7−4.1 deg min^{-1} with each scan recorded in 96 steps, with the outermost 16 steps on each end of the scan being used for background determination. Three standard reflections were monitored at 60 min intervals of X-ray exposure with minor variations in intensity being observed; data were not corrected. An absorption correction was applied based upon crystal faces with transmission factors ranging from 0.8268 to 0.9615. Four data forms were collected that included the indices $-h \pm k \pm l$, resulting in the measurement of 8299 reflections, 3906 unique [R(int) = 0.1110]. Data for compounds **4**−**6** were collected in a similar fashion with the corresponding variables listed in Table 1.

All crystallographic calculations were performed on a personal computer with dual Pentium 450 MHz processors and 256 MB of extended memory. Data were corrected for Lorentz and polarization factors and reduced to F_o^2 and $\sigma(F_o^2)$ using the program XCAD4.[18] For all structures, XPREP[19] was used to check cell symmetry and create the initial SHELX files. For **3**, this procedure confirmed the unique noncentrosymmetric orthorhombic space group $P2_12_12_1$ (no. 19), while in the case of **4**, systematic absences clearly determined the centrosymmetric monoclinic space group $P2_1/n$ (no. 14), nonstandard setting for $P2_1/c$. For **5**, this procedure once more confirmed the unique noncentrosymmetric orthorhombic space group $P2_12_12_1$ (no. 19), while for **6**, systematic absences indicated the centrosymmetric space group *Pnma* (no. 62), or the noncentrosymmetric space group $Pna2_1$ (no.33), with intensity statistics clearly favoring the centric case. All structures were then determined by direct methods using the program XS,[20] which resulted in the successful location of nearly all nonhydrogen atoms comprising the molecule. The remaining nonhydrogen atoms were located from two subsequent difference Fourier maps. Finally, the structures were refined with XL.[21] Hydrogen atoms were placed in calculated positions, these being dependent on both the type of bonding at the carbon and temperature, with aromatic d(C−H) = 0.950 Å with U_H equal to $1.2U_{(parent)}$, tertiary d(C−H) = 0.98, and the methyl hydrogens being initially located via a circular difference Fourier about the individual carbon atom with d(C−H) = 0.96 Å, $U_H = 1.5U_{(parent)}$. All of the non-hydrogen atoms were refined anisotropically, and the structures were refined to convergence. All of the hydrogen atoms were allowed to refine freely (*xyzU*). For compounds **3** and **5**, the absolute structure parameters were also refined, Flack(x) = −0.01(5) for **3** and Flack(x) = −0.03(3) for **5**, indicating that these structures are both correct and complete.[22]

Supporting Information Available: Variable-temperature ^{1}H NMR spectra for **5** and details of the structure determinations and crystallographic data for complexes **3**−**6**, including complete listings of atom positions, isotropic and anisotropic temperature factors, and bond distances and bond angles. This material is available free of charge via the Internet at http://pubs.acs.org.

OM990481Z

(17) *CAD-4 EXPRESS*, Version 5.1/1.2; Enraf-Nonius: Delft, The Netherlands, 1994.

(18) Harms K. *XCAD4*, Program for the Lp-correction of Nonius-CAD-4 diffractometer data; University of Marburg: Germany, 1997.

(19) . Sheldrick, G. M. *SHELXTL*, Version 5.03; Siemens Analytical X-ray Instruments Inc.: Madison, WI, 1994.

(20) Sheldrick, G. M. *Acta Crystallogr.* **1990**, *A46*, 467−473.

(21) Sheldrick, G. M. *SHELXL-93*, Program for the Refinement of Crystal Structures; University of Göttingen: Germany, 1993.

(22) Flack, H. D. *Acta Crystallogr.* **1983**, *A39*, 876−881.